

High-Momentum-Transfer Inelastic Neutron Scattering from Liquid Helium-3

P. E. Sokol^(a)

Department of Physics, University of Illinois at Urbana-Champaign, Urbana, Illinois 61801

and

K. Sköld

The Studsvik Science Research Laboratory, S-61182 Nyköping, Sweden

and

D. L. Price and R. Kleb

Materials Science and Technology Division, Argonne National Laboratory, Argonne, Illinois 60439

(Received 9 August 1984)

The inelastic scattering of neutrons by liquid ^3He at 0.2 K saturated vapor pressure has been measured for momentum transfers in the range $10 \text{ \AA}^{-1} < Q < 16 \text{ \AA}^{-1}$. The observed scattering function is well described, within statistical uncertainties, by a Gaussian centered at the recoil energy. The average kinetic energy per atom, obtained from the width of the scattering function, is 8.1 ± 1.7 K.

PACS numbers: 67.50.Dg, 61.12.Fy

Liquid ^3He at low temperatures is a degenerate Fermi liquid of considerable experimental and theoretical interest. One of the unique features of degenerate Fermi systems is that the single-particle momentum distribution $n(\mathbf{p})$ has a discontinuity at the Fermi energy E_F if the interaction between the particles is not too strong. A direct observation of $n(\mathbf{p})$ would be of great help in evaluating theoretical calculations of the ground state in the liquid. In the absence of a direct observation of the shape of $n(\mathbf{p})$, information on the moments, one of which gives the average kinetic energy per atom, is of great use since they may be compared to theoretical calculations.

Information about $n(\mathbf{p})$ can be obtained from inelastic neutron scattering experiments. At sufficiently large values of the momentum transfer Q , only single-particle scattering is observed. The dynamic structure factor $S(\mathbf{Q}, E)$ may then be calculated using the impulse approximation (IA) and is given by

$$S(\mathbf{Q}, E) = \int n(\mathbf{p}) \delta\left(E - \frac{\hbar^2 Q^2}{2M} - \frac{\hbar^2}{M} \mathbf{Q} \cdot \mathbf{p}\right) d^3p, \quad (1)$$

where M is the mass of the particles constituting the scattering system. Recent measurements¹ on liquid and solid ^4He have shown that the IA is valid for momentum transfers above 10 \AA^{-1} and that the single-particle momentum distribution may be obtained from the observed $S(\mathbf{Q}, E)$. Analogous experiments using x rays have been made to study $n(\mathbf{p})$ of electrons in metals and have observed the discontinuity at the Fermi surface.²

We report here the first neutron scattering measurements on liquid ^3He at high momentum transfer. The experiment was carried out with the low-resolution medium-energy chopper spectrometer (LRMECS) at the Intense Pulsed Neutron Source at Argonne.

LRMECS is a time-of-flight spectrometer with a chopper before the sample to monochromatize the pulsed white beam from the spallation neutron source. The chopper-source phasing was chosen such that neutrons of energy 260 meV were selected. Time-of-flight spectra for scattered neutrons were observed at fourteen scattering angles between 58.8° and 116.4° , corresponding to momentum transfers in the range 10 \AA^{-1} to 16 \AA^{-1} for neutrons scattered from freely recoiling ^3He atoms.

The large neutron-absorption cross section of the ^3He nucleus complicates the experiment, because to correctly remove the scattering from the cell we must be able to do an empty-cell run without observing scattering from the parts of the cell obscured by the sample. The optimal configuration in this case is to

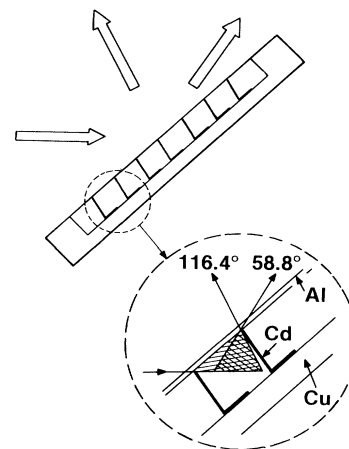


FIG. 1. Cell geometry used in this work; the inset illustrates how the cadmium slats prevent scattering from the back of the cell from reaching the detectors.

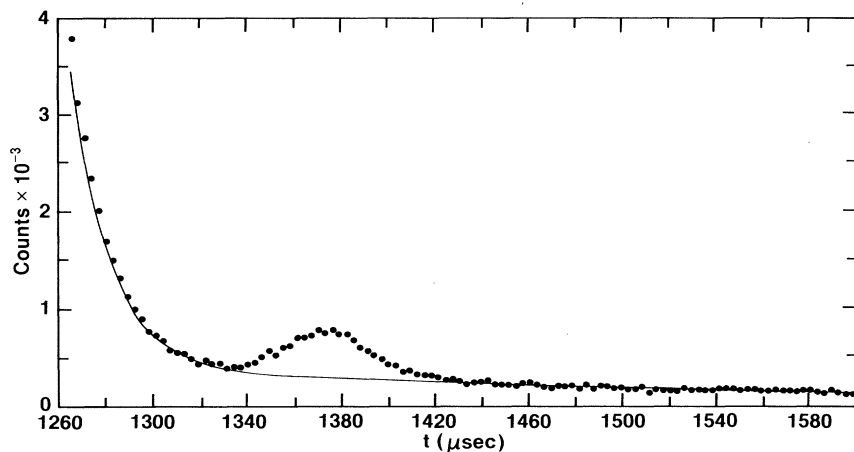


FIG. 2. Observed scattering with (circles) and without (line) the ^3He sample in the cell at 91.8° scattering angle. The large signal at small times is due to scattering from the Al window.

use a reflection geometry and a cell design of the type used by Sköld and Pelizzari³ which makes use of cadmium slats to shield the back of the cell from the detectors. The body of the present cell was made of copper with an aluminum front window, 0.8 mm thick, glued to the copper. The normal to the cell was oriented at 45° to the incident beam. The sample cell and the scattering geometry are illustrated in Fig. 1. With this arrangement extraneous scattering from the Al window is minimized, while no scattering is observed from the back of the cell when the sample is not present.

The sample cell was attached to the mixing chamber of a ^3He - ^4He dilution refrigerator which maintained the sample temperature T at 0.20 K. The liquid was at saturated vapor pressure (SVP). At this density, the Fermi temperature⁴ is $T_F = 1.6$ K. Since $T \ll T_F$, the difference from a measurement at the $T = 0$ should be

insignificant.

Data were collected for 103 h on the ^3He sample and for 24 h on the empty cell. The time-average flux on sample was 5.5×10^3 n/cm^2 s. Examples of the spectra observed with the filled cell and with the empty cell are shown in Fig. 2. The main contribution to the background is the scattering from the Al window. Due to the relatively large mass of aluminum, this contributes a signal at energies below the recoil peak from ^3He . The scattering from the cell is approximately 1 order of magnitude larger than the ^3He signal. The same data are shown in Fig. 3 after correction for the cell scattering and detector efficiency and after conversion to $S(Q, E)$ form. No correction has been made here for self-absorption in the sample since this is relatively constant over the energy range covered by the recoil peaks. Also, no correction has been made for multiple scattering: Because of the highly absorbing

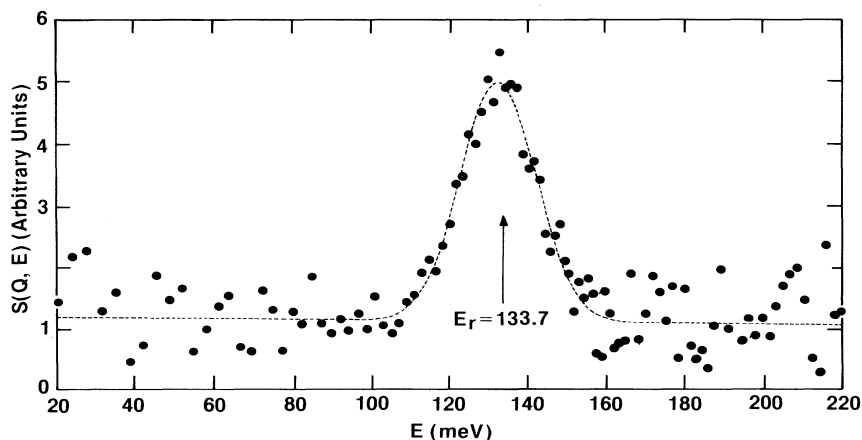


FIG. 3. Scattering function $S(\phi, E)$ at 91.8° scattering angle. The momentum transfer is $Q = 13.85 \text{ \AA}^{-1}$. The arrow marks the recoil energy for neutron scattering from a ^3He nucleus. The dotted line is a fit to the data with a Gaussian.

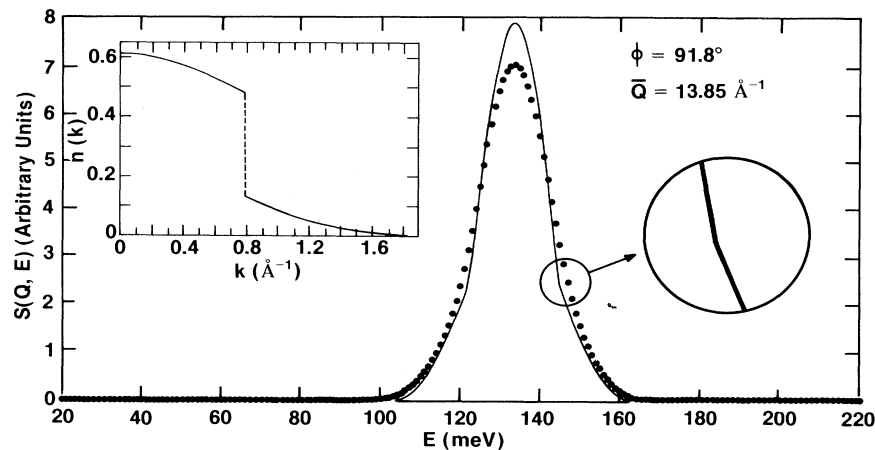


FIG. 4. Ideal (line) and resolution broadened (circles) scattering from liquid ${}^3\text{He}$ calculated using the momentum distribution (inset) from Ref. 5.

sample, this is mainly confined to Al- ${}^3\text{He}$ and ${}^3\text{He}$ -Al double scattering events, which contaminate the signal by approximately 1%. The absence of any significant signal at small energy transfer after the background subtraction provides a valuable check on our data-reduction procedures. The large statistical errors at low energy result from the subtraction of the large cell scattering. The fluctuations at large energy transfer result from the conversion from time-of-flight spectrum to $S(Q, E)$.

In Fig. 4 we show a theoretical scattering function evaluated from Eq. (1) using $n(p)$ obtained by Lam *et al.*⁵ at $T=0$, at constant scattering angle and for an incident neutron energy of 260 meV. The structure in $n(p)$, in particular the discontinuity at the Fermi surface, is displayed in the theoretical scattering function. However, after folding this with a Gaussian of width equal to the resolution of the present experiment for the data shown in Fig. 3, the curve shown by the solid circles in Fig. 4 is obtained. Finite-temperature effects also broaden $n(p)$; we estimate that this broadening is approximately 0.02 meV under our experimental conditions. Clearly, under the present experimental conditions the relevant structure in the scattering function is not resolved. The statistical accuracy of the present experiment precludes a detailed analysis of the shape of the scattering function.

In view of these experimental limitations, the objective of the present work is to extract the lowest-order moments of $S(Q, E)$. To do this, we have fitted a Gaussian function

$$S^*(\phi, E) = A_\phi \exp[-(E - E_\phi)^2 / 2\sigma_\phi^2] \quad (2)$$

to the experimental scattering function at constant angle. A linear function is added to the Gaussian to account for this remaining, nearly constant, background in the corrected data. An example of a typical fit to

the data is shown by the dashed curve in Fig. 3. Within the statistical error the fitted function agrees well with the experimental results, and the parameter E_ϕ agrees with the expected recoil energy for free ${}^3\text{He}$ atoms. If $S(Q, E)$ at constant Q can be represented by a Gaussian of width σ_Q , the average kinetic energy per atom $\langle K \rangle$ is obtained from the expression

$$\sigma_Q = Q(2\hbar^2 \langle K \rangle / 3M)^{1/2}. \quad (3)$$

The constant-angle data for the dynamic structure factor have been transferred to constant Q and corrected for experimental resolution using procedures described in Ref. 1. The values of σ_Q thus obtained are shown in Fig. 5, together with a fit with the straight line given by Eq. (3). The kinetic energy obtained from this fit is

$$\langle K \rangle = 8.1 \pm_{1.3}^{1.7} \text{ K}.$$

We note that $\langle K \rangle$ can also be obtained from the sum rule⁶

$$\langle K \rangle = \frac{\int_{-\infty}^{\infty} (E - E_r)^2 S(Q, E) dE}{\frac{4}{3} E_r} \quad (4)$$

which does not rely on the validity of the IA. For coherent scattering, Eq. (4) is valid only in the high- Q limit where interference effects vanish; however, such effects are too small to be observed under the conditions of this experiment. Evaluation of $\langle K \rangle$ from the present experimental results using Eqs. (3) and (4) yields the same results within statistical uncertainty, although the evaluation of $\langle K \rangle$ from Eq. (4) leads to much larger errors due to the relatively poor statistics.

There have been several calculations of $\langle K \rangle$ using cluster expansion,⁵ variational,⁷ and Green's function Monte Carlo⁸ techniques. These calculations, using Lennard-Jones potential and the correctly symmetrized wave function, obtain values of $\langle K \rangle$ in the

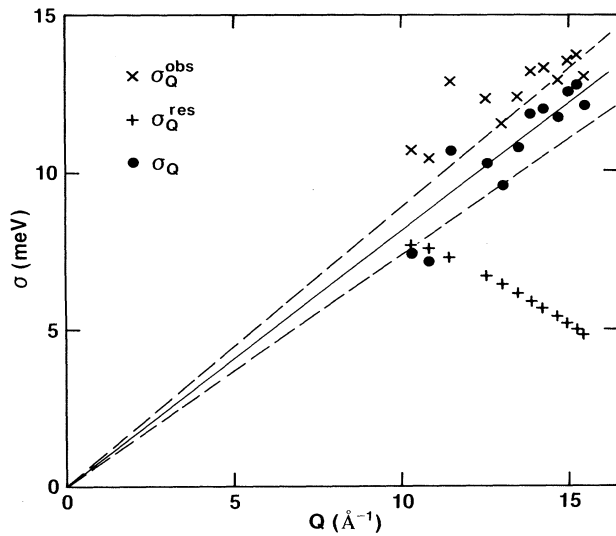


FIG. 5. Widths σ_Q of the Gaussian fit to the data at constant Q before (crosses) and after (circles) correction for resolution. The experimental resolution width is also shown (pluses). The solid line represents a least-squares fit of Eq. (3) to the data and the dashed lines are one standard deviation from the fit.

range 7 to 10 K. A more recent calculation⁹ obtained $\langle K \rangle = 13$ K.

This work was supported by the U. S. Department of Energy, Division of Materials Sciences, under Contracts No. DE-AC02-76ER01198 and No. W-31-109-

ENG-38, and by the Division of Educational Programs at Argonne.

(a)Permanent address: Department of Physics, Harvard University, Cambridge, Mass. 07138.

¹R. O. Hilleke, P. Chaddah, R. O. Simmons, D. L. Price, and S. K. Sinha, Phys. Rev. Lett. **52**, 847 (1984); P. E. Sokol, R. O. Simmons, D. L. Price, and R. O. Hilleke, in *Proceedings of Seventeenth International Conference on Low Temperature Physics, Karlsruhe, Germany, 1984* (North-Holland, Amsterdam, 1984).

²W. C. Phillips, and R. J. Weiss, Phys. Rev. **171**, 790 (1968).

³K. Sköld and C. A. Pelizzari, Philos. Trans. Roy. Soc., Ser. B, **290**, 305 (1980).

⁴W. E. Keller, *Helium 3 and Helium 4* (Plenum, New York, 1969), p. 216.

⁵P. M. Lam, H. W. Jackson, M. L. Ristig, and J. W. Clark, Phys. Lett. **58A**, 454 (1976); P. M. Lam, J. W. Clark, and M. L. Ristig, Phys. Rev. B **16**, 222 (1977).

⁶G. Placzek, Phys. Rev. **86**, 377 (1952); A. Rahman, K. S. Singwi, and A. Sjölander, Phys. Rev. **126**, 986 (1962); E. Feenberg, *Theory of Quantum Fluids* (Academic, New York, 1969), p. 83.

⁷D. Ceperly, G. V. Chester, and M. H. Kalos, Phys. Rev. B **16**, 3081 (1977); K. E. Schmidt, M. A. Lee, M. H. Kalos, and G. V. Chester, Phys. Rev. Lett. **47**, 807 (1981).

⁸M. A. Lee, K. E. Schmidt, M. H. Kalos, and G. V. Chester, Phys. Rev. Lett. **46**, 728 (1981).

⁹R. M. Panoff, private communication.